

PCCP

Accepted Manuscript



This is an *Accepted Manuscript*, which has been through the Royal Society of Chemistry peer review process and has been accepted for publication.

Accepted Manuscripts are published online shortly after acceptance, before technical editing, formatting and proof reading. Using this free service, authors can make their results available to the community, in citable form, before we publish the edited article. We will replace this *Accepted Manuscript* with the edited and formatted *Advance Article* as soon as it is available.

You can find more information about *Accepted Manuscripts* in the [Information for Authors](#).

Please note that technical editing may introduce minor changes to the text and/or graphics, which may alter content. The journal's standard [Terms & Conditions](#) and the [Ethical guidelines](#) still apply. In no event shall the Royal Society of Chemistry be held responsible for any errors or omissions in this *Accepted Manuscript* or any consequences arising from the use of any information it contains.

**Extensive Theoretical Studies on Two New members of the FOX-7 family:
5-(dinitromethylene)-1,4-dinitramino-Tetrazole and
1,1'-dinitro-4,4'-diamino-5,5'-Bitetrazole as Energetic Compounds**

*Piao He^a, Jian-Guo Zhang^{*a}, Kun Wang^{ab}, Xin Yin^a, Xin Jin^a, Tong-Lai Zhang^a*

^aState Key Laboratory of Explosion Science and Technology, Beijing Institute of Technology, Beijing 100081 P. R. China;

^bDepartment of Chemistry, Inorganic Chemistry Laboratory, University of Oxford, South Parks Road, Oxford OX1 3QR, United Kingdom

Abstract: Two novel compounds 5-(dinitromethylene)-1,4-dinitramino-Tetrazole (DNAT) and 1,1'-dinitro-4,4'-diamino-5,5'-Bitetrazole (DNABT) were suggested to be potential candidate of high energy density materials (HEDM). The optimized geometry, NBO charges and electronic density, HOMO-LUMO orbital, electrostatic potential on surface of molecule, IR spectrum and thermochemical parameters were calculated for inspecting the electronic structure properties with B3LYP/6-311++G** level of theory. Meanwhile, the solid state of DNAT and DNABT were studied using the crystal packing models with the plane-wave periodic local-density approximation density functional theory. Four stable polymorphous cells have been found including P_{212121} , $P_{21/C}$, P-1 and P_{BCA} , assigned to the orthorhombic, monoclinic and triclinic lattice systems. In addition, properties such as density, enthalpy of formation and detonation performance have been also predicted. As a result, the detonation velocity and pressure of two compounds are very remarkable (DNAT: $D = 9.17$ km/s, $P = 39.23$ GPa; DNABT: $D = 9.53$ km/s, $P = 40.92$ GPa). Considering the tetrazole rings with energetic groups and the insensitive fragment of FOX-7, high positive heat of formation (583.50 kJ/mol and 1081.39 kJ/mol) and eminent performance, render DNAT and DNABT to be very promising powerful energetic insensitive compounds. This work provides the theoretical support for further experimental synthesis.

Key words: Density functional theory (DFT); 5-(dinitromethylene)-1,4-dinitramino-tetrazole (DNAT); 1,1'-dinitro-4,4'-diamino-5,5' bitetrazole (DNABT); Enthalpy of formation; Detonation performance

* The type of article: Research paper

Corresponding authors: Jian-Guo Zhang, Tel & Fax: +86 10 68918091.

E-mail: zjgbit@bit.edu.cn

1. Introduction

Energetic materials include explosives, propellants, and pyrotechnics that are used for a variety of military purposes and civilian applications.¹ Much attention is focused on designing new and improved high energy density materials (HEDMs) that exhibit a good balance between sensitivity and performance. However, the demands of high energy and insensitivity are quite often contradictory to each other, making the development of novel HEDMs a challenging problem.²

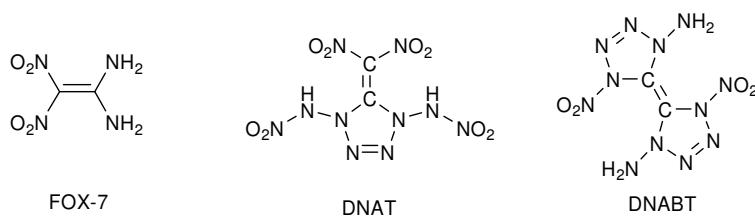
High-nitrogen compounds constitute a unique class of energetic materials and have received a substantial amount of interests due to their favorable insensitivity, good explosive performance, and environmental acceptability.³⁻⁸ Tetrazoles are an important core of aza-containing heterocycles because of practical and theoretical significance and diversity of their characteristics (high nitrogen content, high heats of formation and good thermal stability), which makes these compounds may be of high density, releasing considerable energy and gases upon decomposition/explosion.⁹⁻¹⁷ Meanwhile, the physical and explosive properties of tetrazole derivatives are rather easily modified by the replacement of substituents with various functional groups.

1,1-Diamino-2,2-dinitroethylene (FOX-7), first synthesized in 1999,¹⁸ was established as a less sensitive, high-performance explosive and has emerged as a potential candidate to replace the secondary explosive RDX (cyclo-1,3,5-trimethylene-2,4,6-trinitramine)¹⁹ because of its potentially high performance ($D = 8.930$ km/s, $\rho = 1.88$ g·cm⁻³), thermal stability, and low sensitivity to impact and friction. FOX-7 is a representative nitro-enamine compound, which possesses a highly polarized carbon-carbon double bond with positive and negative charges being stabilized by the amino group and nitro group respectively. Many researches such as synthetic methods, structure modification and theoretical studies focused on FOX-7 have attracted considerable attention.²⁰⁻²⁸ Some of these documented materials exhibit impressive energetic properties, which motivated us to design new energetic compounds based on derivatives of FOX-7.

The often prohibitive time and cost as well as danger associated with the synthesis and testing of a new energetic material have driven the advancement of computationally assisted development of HEDMs.²⁹ To meet the continuing demand for improved energetic materials, there is a clear need to continue to design and develop new candidates with high explosive performance and insensitivity. Attempt to introduction of the tetrazole ring may design a new kind of the derivatives based on FOX-7 that containing nitramine group and gem-dinitro group as important contribution of rich

energy and high density. It is not surprising that the combination of interesting energetic properties and unusual chemical structures has attracted us to this unique class of compounds.

In this work, we first reported 5-(dinitromethylene) -1,4-dinitramino-Tetrazole (in short DNAT) and 1,1'-dinitro-4,4'-diamino-5,5'-Bitetrazole (in short DNABT) as two new members of the FOX-7 family. (Scheme 1) The electronic structure, enthalpy of formation, crystal packing mode and density, and detonation performance of DNAT and DNABT, have been studied rigorously. The present theoretical study may simulate further experimental study of these two novel high-nitrogen energetic compounds including synthesis and testing.



Scheme 1 The designed compounds as new members of the Fox-7 family

2. Computational methods

The geometry of DNAT and DNABT have been optimized using the hybrid DFT-B3LYP method with the 6-311++G** basis set. Harmonic vibrational frequencies including the IR spectrum and thermochemical parameters were obtained at the same levels of theory. Meanwhile, the electronic properties, natural bond orbital (NBO) charges, the highest occupied molecular orbitals (HOMO) and the lowest unoccupied molecular orbital (LUMO) orbitals, and electrostatic potential on molecular surface of the title compounds were calculated on the B3LYP/6-311++G** level of theory based on the optimized gas-phase structure.

Enthalpy of formation is the most important parameter for energetic compounds. Atom equivalent schemes are used to convert quantum mechanical energies of formation of atoms to heats of formation for various classes of molecules. The gas-phase heat of formation using atom equivalents is represented as³⁰:

$$\Delta H_f(g) = E(g) - \sum_i n_i x_i \quad (1)$$

In Eq. (1), $E(g)$ is the computed minimum energy of the molecule at 0 K, n_i is the number of atoms of element i and x_i is its atom equivalent energy. We have used the x_i determined by Rice and Byrd through a least-squares fitting of Eq. (1) to the experimental $\Delta H_f(g)$ of a series of C, H, N, O-containing energetic compounds.³⁰

Often the standard state of the material of interest corresponds to the condensed phase. Thus, Condensed-phase heats of formation can be determined using the gas-phase enthalpy of formation and enthalpy of phase transition (either sublimation or vaporization) according to Hess' law of constant heat summation³¹:

$$\Delta H(\text{Solid}) = \Delta H(\text{Gas}) - \Delta H(\text{Sublimation}) \quad (2)$$

$$\Delta H(\text{Liquid}) = \Delta H(\text{Gas}) - \Delta H(\text{Vaporization}) \quad (3)$$

Based on the electrostatic potential of molecule through quantum mechanical prediction, the heat of sublimation either vaporization can be represented as^{32, 33}:

$$\Delta H(\text{Sublimation}) = a(\text{SA})^2 + b\sqrt{\sigma_{\text{Tot}}^2 v} + c \quad (4)$$

$$\Delta H(\text{Vaporization}) = a\sqrt{(\text{SA})} + b\sqrt{\sigma_{\text{Tot}}^2 v} + c \quad (5)$$

Where (SA) is the molecular surface area for this structure, σ_{Tot}^2 is described as an indicator of the variability of the electrostatic potential on the molecular surface, and v is interpreted as showing the degree of balance between the positive and negative potentials on the molecular surface. And where a , b , and c are fitting parameters. We further followed the approach of Politzer et al. to predict the heats of sublimation and vaporization then combined these with Eq. (2) or Eq. (3) to predict solid and liquid enthalpy of formation.

Besides enthalpy of formation, the other critical parameter for energetic material is the crystal packing density. About 80% organic crystals possess symmetries belong to the space groups P21/C, P-1, P212121, P21, C2C, and PBCA, respectively.²⁹ Therefore, the six types of crystals were chosen as candidates for DNAT and DNABT packing. The periodic density functional calculation was carried out using the plane-wave local density approximation (LDA).³⁴ The ultrasoft pseudopotentials were used with an energy cutoff of 340 eV. For the integration over the Brillouin zone, the special k-points were chosen using the Monkhorst-Pack grid of 3×3×3. In the optimizations, the maximum force, displacement, stress component, and the total electronic energy were converged to within 0.03 eV/Å, 0.001 Å, 0.05 GPa, and 1×10⁻⁵ eV/atom, respectively.

The empirical Kamlet-Jacob equations³⁵ widely employed to evaluate the energy performance of energetic compounds were used to estimate the detonation velocity and detonation pressure of title compound. Empirical Kamlet-Jacobs equations can be written as follows:

$$D = 1.01 \left(N \bar{M}^{-1} Q^{\frac{1}{2}} \right)^{\frac{1}{2}} (1 + 1.30\rho) \quad (6)$$

$$P = 1.558\rho^2 N \bar{M}^{\frac{1}{2}} Q^{\frac{1}{2}} \quad (7)$$

Where D is the detonation velocity (km/s); P is the detonation pressure (GPa); N is the moles of detonation gases per gram explosive; \bar{M} is the average molecular weight of these gases; Q is the heat of detonation (cal/g); and ρ is the loaded density of explosives (g/cm³). In practice, the loading density can only be approximated to a value less than the theoretical density, thus the D and P values obtained from Eq. 6 and Eq. 7 can be regarded as their upper limits.

All the calculations involved in this work were carried out using the Gaussian 09 program package.³⁶ The crystal prediction was performed using the Materials Studio programs.³⁷

3. Results and Discussion

3.1 Molecular Structure

In generally, the differences in electronic energy in the gas phase were used to determine the most probable geometry of designed new compounds from many conformations. The most stable molecule conformations of DNAT and DNABT retain planar-ring structure of the tetrazole, as shown in Fig. 1. The selected geometry parameters of optimized molecules are listed in Table 1(Supporting Information 1).

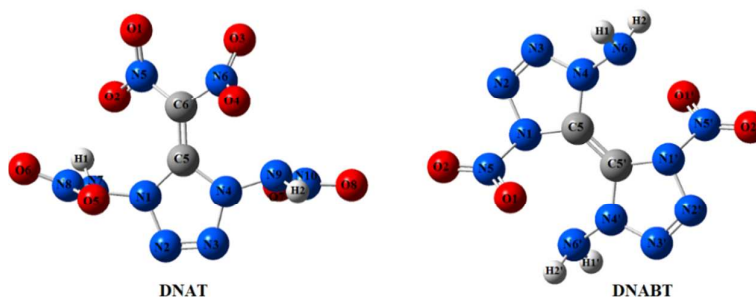


Fig. 1 The optimized geometry of DNAT and DNABT

It is evident that tetrazole ring and carbon-carbon double bonds construct the whole main body of molecules both in DNAT and DNABT. And in the rings, all N atoms and C atom are in the same plane and the bonding angles of ring atoms are about 108°. The length of N=N bond is shorter than that of C=C bond due to the diverse electronegativity. For the compound DNAT, there are conjoint directly eight nitrogen atoms and molecular structure is not symmetry. Four nitro are arranged beside the tetrazole ring with a certain angles because of the electron repulsion among oxygen atoms. While the other DNABT with six catenated nitrogen atoms, possesses double tetrazole rings

linked by the stable C=C bond. And two nitro and two amino are cross arranged around ring, forming the centro-symmetric configuration. Again the effect of lone pair electrons both on the nitrogen and oxygen atoms, makes the nitro and amino deviating from the tetrazole-ring plane, implying that the electronic properties play a key role for the molecular structure of our concern.

3.2 Electronic Density and Charges

A fundamental concept in chemistry is that a variety of atomic and molecular properties can be expressed in terms of the electronic density population. Using the Multiwfn program³⁸ calculating density, the contour line maps of electronic density on DNAT and DNABT are visualized in Fig. 2.

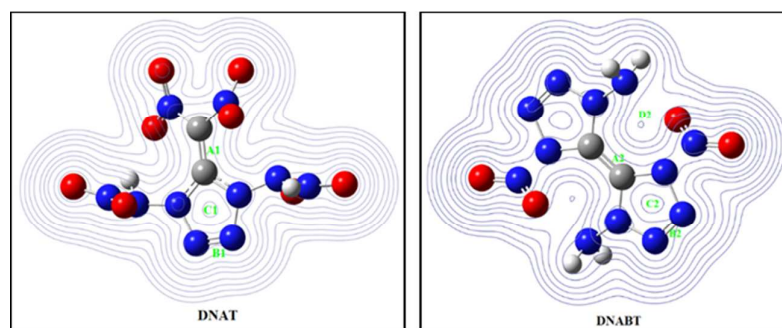


Fig. 2 Contour line map of electronic density on DNAT and DNABT

Firstly the heavy nucleus has high peaks caused by nuclear charge improving electron aggregation and then displays integral exponential attenuation towards all around. And the electron densities surrounding the oxygen and nitrogen atoms are higher than that of other atoms due to the strong electronegativity. Generally electrons prefer to assemble in the bonding area (such as A1, A2, B1 and B2) because of electron pair sharing between atoms with covalence interaction. And this suggests their nature of purely covalent bonding derived from the π orbitals and electrons delocalized over the C=C and N=N bonds. Moreover, the delocalization also occurs in tetrazole ring, as marked C1 and C2, which may improve the stability of the ring skeleton as well as molecular structure. Again for DNABT, the repulsive interactions of lone pair electrons among the adjacent atoms lead naturally reduction of electronic density (as shown in D2 region), and two nitro and amino have been discarded as expected. Both DNAT and DNABT are stabilized by involving the lone pairs of alternate nitrogen atoms in coordinate covalent bonds to carbon atoms, and this presumably reduces the destabilizing repulsion between adjacent lone pairs.

Natural Bond Orbital (NBO) charges are considered more reasonable for discussion, exactly

what was suggested in Table 2(Supporting Information 2). Observed for the molecule DNAT, the N1 and N4 atoms as well as N7 and N9 atoms display negative charges, while the N2 and N3 atoms show positive charge unexpectedly due to the inductive effect of $-\text{NO}_2$ as electron-withdrawing group. And the N5, N6, N8 and N10 atoms in nitro group accommodate higher positive charges because of the strong electronegativity on oxygen, making much electron departure towards the oxygen atom. It is worth noticing that the characteristic of symmetric distribution on atomic charges of DNABT, which agrees with the centro-symmetric molecular configuration.

3.3 Frontier Molecular Orbitals (FMOs)

The highest occupied molecular orbitals (HOMOs) and the lowest unoccupied molecular orbitals (LUMOs) are named as frontier molecular orbitals (FMOs). The energy gap between HOMO and LUMO determines the kinetic stability, chemical reactivity and optical polarizability and chemical hardness-softness of a molecule.³⁹ The HOMO and LUMO orbitals including the energy gap are depicted in Fig. 3.

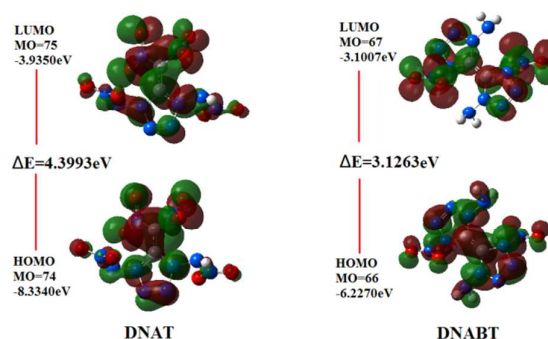


Fig. 3 HOMO and LUMO orbitals of DNAT and DNABT

It is clear from the figure that, the HOMO of DNAT molecule is localized approximately on the tetrazole ring and the π orbitals are mainly distributed the C=C bond and N=N bond with the typical covalent nature. With respect of DNABT, the HOMO is localized in the double rings of tetrazole. It is similar to DNAT that the carbon-carbon double bond and nitrogen-nitrogen double bond exhibit characteristic of the π electrons aggregation. Moreover, the LUMO is localized on nitro group and scarcely on the amino group. In addition, the HOMO \rightarrow LUMO transition implies an electron density transfer from donator to acceptor. The calculated value of energy separation between the HOMO and LUMO is 4.3993 eV and 3.1263 eV respectively. And this allows the molecular orbitals to overlap to have a proper electronic communication conjugation, which is a

marker of the intramolecular charge transfer from the electron donating group through the π -conjugation system to the electron accepting group.

3.4 Electrostatic potential on molecular surface

Electrostatic potential (ESP) on molecular surface is critical for understanding intermolecular interaction and gives more meaningful insight into charge distributions.⁴⁰ The ESP mapped vdW surface of DNAT and DNABT are shown in Fig. 4. Significant surface local minima and maxima of ESP are represented as orange and cyan spheres, and labelled by dark blue and brown-red texts, respectively. The unit is in kcal/mol. Only the global minima and maxima on the surface are labelled by italic font. The surface areas in each ESP range are plotted as Fig. 5.

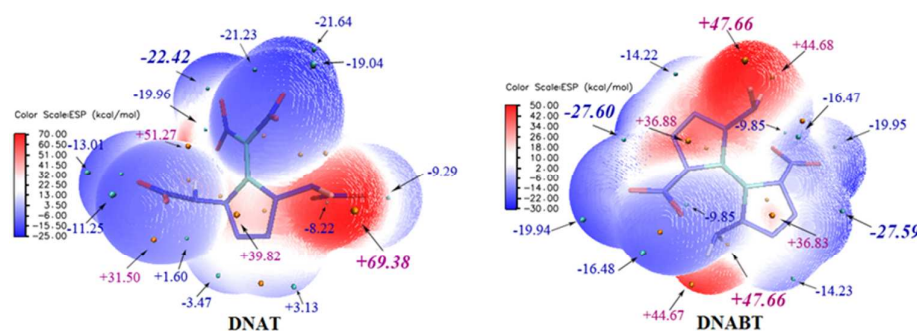


Fig. 4 ESP mapped molecular vdW surface of DNAT and DNABT

It can be seen that in the DNAT unit region, the surface minima of ESP display between oxygen atoms because of higher electronegativity itself, especially on the O1, O2, O3 and O4 of nitro joint to the carbon atom, which are the primary electrophilic sites. While the surface maximum prefer to carbon and hydrogen atoms, which illustrates that the electrostatic potential is dominated by nuclear charge and may be attacked easily by the nucleophile. It is similar to the DNABT unit, the surface maximum of ESP are distributed near hydrogen atoms (H1, H2) and the minima are distributed oxygen atoms (O1, O2), respectively. The global maxima of ESP on the DNAT and DNABT surface are +69.38 and +47.66 kcal/mol corresponding to the hydrogen, while minima are -22.42 and -27.60 kcal/mol corresponding to the oxygen. These observations are consistent with the atomic charges from foregoing natural bond orbital analysis.

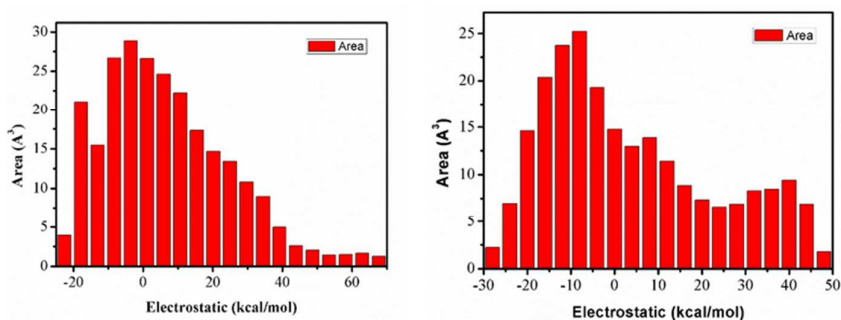


Fig. 5 Area percent in each ESP range of DNAT and DNABT

For the DNAT unit from Fig. 5, most parts of surface have low ESP value (i.e. within -20 to +30 kcal/mol), and the biggest area is about -5 kcal/mol, corresponding to the tetrazole ring. The small area of surface ESP at -20 kcal/mol corresponds to the nitro group and another portion surface with value of ESP (i.e. >+45 kcal/mol) corresponds to the hydrogen atom of nitramino group. And the double tetrazole rings are the main contributors to the primary surface area of DNABT unit having ESP value within -25 to +45 kcal/mol. A tiny part of the surface has ESP value larger than +45 kcal/mol stemming from the hydrogen, and another surface has value smaller than -25 kcal/mol contributed of the oxygen.

3.5 Vibration Analysis

IR spectrum is an effective method to identify the substances and it is quite related to the thermodynamics properties. The simulated infrared spectra of DNAT and DNABT are shown in Fig. 6. The horizontal axis represents frequency and the vertical axis denotes intensity, respectively.

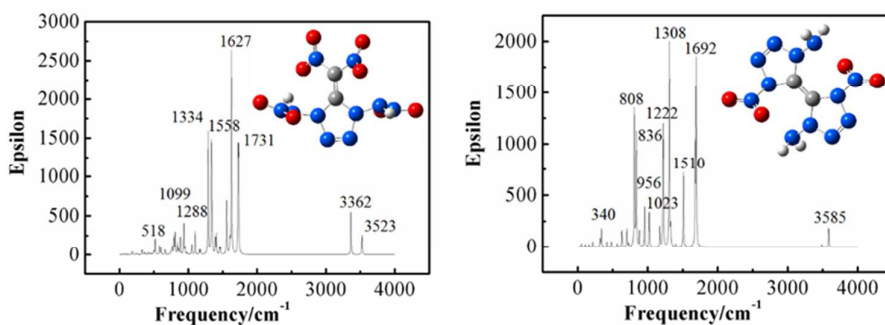


Fig. 6 Calculated IR spectrum of DNAT and DNABT

The calculated IR results show that the strongest IR peaks at 1627 cm^{-1} of DNAT compound corresponds to the symmetrical stretching modes in the carbon- carbon double bonds. The region in 3523 cm^{-1} and 3362 cm^{-1} belong to stretching vibration of N-H bond and the peaks at 518 cm^{-1} are

rocking modes in the nitramino group. The stronger one at 1558 cm^{-1} and 1099 cm^{-1} refer to symmetrical stretching of N=N bond and symmetrical stretching of C-N bond in the tetrazole ring, while the peaks at 1731 cm^{-1} belongs to the scissor vibration mode of N-H bond. And the N-O bonds in the nitro group have different peaks at 1228 cm^{-1} and 1334 cm^{-1} , referring to symmetrical stretching vibrations. Meanwhile, the DNABT compound has two strongest IR peaks at 1308 cm^{-1} and 1692 cm^{-1} , which are the symmetrical and asymmetrical stretching modes in nitro group and the scissor vibration mode in amino group, respectively. The amino group was observed vibration modes along with additional three characteristic peaks in the IR spectrum at 3585 cm^{-1} , 340 cm^{-1} and 836 cm^{-1} refer to the asymmetrical stretching and the torsion modes as well as the N-H bending and out-of-plane deforming. The stronger peaks at 1510 cm^{-1} and 1222 cm^{-1} are assigned to the stretching modes of the N=N bond and the C=C bond, respectively. While the peak at 1023 cm^{-1} and 951 cm^{-1} as medium peaks are mainly dominated by stretching vibration on C-N and N-N of tetrazole skeleton. The nitro group also has another vibration modes of torsion ranged in the weak peaks at 808 cm^{-1} . It's worth being noticed that the variances of vibrations on the nitro group and the amino in different positions were observed through value and intension of IR spectrum both in DNAT and DNABT compounds.

On the basis of vibrational analysis and statistic thermodynamic method, thermodynamic functions, such as thermal correction to internal energy (U), enthalpy (H), free energy (G), standard molar heat capacity (C_v) and standard molar thermal entropy (S), as well as zero-point energy (ZPE) of two major compounds were evaluated and tabulated in Table 3. All these values are at 298.25K, 1.00 atm. and with kcal/mol as unit (kcal/(mol·K) for S and C_v).

Table 3 Thermochemical parameters of DNAT and DNABT

Species	ZPE	U	H	G	S	C_v
DNAT	72.90	83.57	84.17	43.11	137.70	59.66
DNABT	82.16	92.15	92.74	54.52	128.20	57.22

3.6 Crystal Packing and Density

The predicted structures for six types of crystals about DNAT and DNABT were optimized by using CASTEP⁴¹ with the periodic LDA density functional theory and are illustrated in Fig. 7.

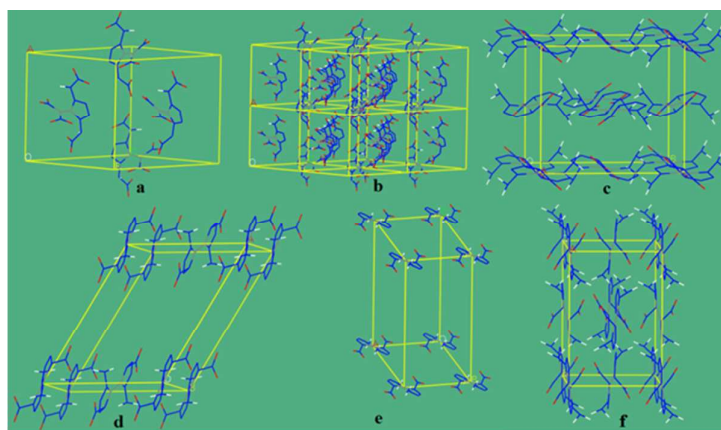


Fig. 7 Unit cells of the DNAT and DNABT crystals calculated using the periodic LDA density functional theory. The crystal structures and packing of DNAT are distribute to letter **a** and **b** in bold and the space group is P_{212121} . The remained **c**, **d**, **e**, and **f** belong to DNABT with the space groups of P_{212121} , $P_{21/C}$, $P-1$ and P_{BCA} , respectively.

The gaseous DNAT molecule is without symmetry so as to the unit-cell being occupied a little molecules in the space group of P_{212121} and the packing structures are depicted in four unit cells as shown in **b**. While DNABT is approximate planar in the crystals to achieve the most significant stacking. After the optimizations using the first-principle plane-wave LDA density functional theory, only four crystals, such as P_{212121} , $P_{21/C}$, $P-1$ and P_{BCA} survive from the six probable crystal types. And they belong to the orthorhombic, monoclinic and triclinic lattice systems. In view of the lattice energy, the more stable crystals belong to the primitive monoclinic ($P_{21/C}$) and orthorhombic (P_{BCA}) lattices. The corresponding crystal structures are shown in [Fig.7](#). And P_{212121} , $P_{21/C}$ and $P-1$ crystals have layered structures, whereas P_{BCA} crystal shows a helix conformation. The remaining cells expand continuously and the molecules become unbound in the end. As a critical parameter for energetic material, the crystal packing density has been estimated to be $1.97 \text{ g}\cdot\text{cm}^{-3}$ for DNAT and $1.85 \text{ g}\cdot\text{cm}^{-3}$ for DNABT, respectively.

3.7 Enthalpy of Formation

If the enthalpy of formation of a proposed explosive is not known experimentally, a number of methods are available for obtaining it computationally at an acceptable level of accuracy, The gas phase heats of formation $\Delta_f H_{298K}(\text{g})$ of DNAT and DNABT were obtained by means of the atom equivalents method. Politzer and coworkers have clearly established that correlations exist between the electrostatic potential of a molecule and its condensed-phase properties, including the heats of sublimation and vaporization. The calculated enthalpies of formation at 298.15K for DNAT and DNABT as well as other common energetic compounds are summarized in [Table 4](#)

Table 4 Enthalpies of Formation, Enthalpy of Vaporization, and Enthalpy of Sublimation (kJ/mol)

Species ^[a]	$\Delta_f H$ (gas)	$\Delta_f H$ (liquid)	$\Delta_f H$ (solid)	ΔH (vap)	$\Delta_f H$ (sub)
TNT ⁴²	24.035	--	-63.12	--	104.50
RDX ⁴²	191.44	--	79.00	--	112.02
HMX ⁴²	--	--	75.24	--	--
FOX-7 ²⁹	--	--	-133.70	--	--
DNAT	727.29	715.23	583.50	12.06	143.79
DNABT	1208.54	1164.29	1081.39	44.25	127.15

^[a] TNT, trinitrotoluene; RDX, cyclotrimethylene trinitramine; HMX, cyclotetramethylene tetranitramine; FOX-7, 1,1-diamino-2,2-dinitroethene.

It is evidently important to use solid state enthalpies of formation in predicting the detonation performance of C, H, N, O compounds. On one hand, some compounds in Table 4 actually have negative enthalpies of formation due to the large enthalpy of phase transition such as TNT and FOX-7. On the other hand, a strongly positive enthalpy of formation is commonly invoked as being very desirable property to increase detonation heat, which is one of the primary reasons for the interest in high nitrogen compounds as explosives. Quite noteworthy in this respect are DNAT and DNABT with the most positive enthalpy of formation (583.50 kJ/mol and 1081.39 kJ/mol) than that of other common energetic compounds and a large enthalpy of formation are very beneficial to the detonation heat so as to improve the detonation velocity and pressure from the theoretical point.

3.8 Detonation Properties

The detonation parameters have been calculated and Table 5 lists the ρ , Q , D , P , and oxygen balance (OB) of title molecules (DNAT and DNABT) and five famous explosives for comparison.

Table 5 Detonation parameters for common HEDMs and two major compounds (DNAT and DNABT)

Species ^[a]	$\Delta_f H_{298K}(s)$ /(kJ/mol)	Q /(cal/g)	ρ /g·cm ⁻³	D /(km/s)	P /GPa	(OB) %
DNAT	583.50	1310	1.97	9.17	39.23	16.32
DNABT	1081.39	1800	1.85	9.53	40.92	-12.30
TNT ⁴³	-63.12	1295	1.64	6.95	19.00	-74.00
RDX ⁴³	79.00	1501	1.80	8.75	34.70	-21.62
HMX ⁴³	102.41	1498	1.90	9.10	39.30	-21.62
FOX-7 ⁴³	-133.70	1200	1.89	8.87	34.00	-21.62
CL-20 ⁴³	377.04	1567	2.04	9.38	44.10	-10.96

^[a] TNT, trinitrotoluene; RDX, cyclotrimethylene trinitramine; HMX, cyclotetramethylene tetranitramine; FOX-7, 1,1-diamino-2,2-dinitroethene; CL-20, hexanitrohexaazaisowuritan.

High density is desirable for energetic materials because more energy will be packed per unit volume. Among these compounds studied here, two new molecules have higher density than that of the traditional explosive such as TNT. And the compound DNAT is worth being noticed with a density of up to $1.97 \text{ g}\cdot\text{cm}^{-3}$, which is similar to excellent CL-20 (value of $2.04 \text{ g}\cdot\text{cm}^{-3}$). Moreover, a large number of inherently energetic C-N and N-N bonds of high-nitrogen molecules benefit the two novel compounds in high positive enthalpy of formation with values of 583.50 kJ/mol and 1081.39 kJ/mol . The OB (oxygen balance) is another parameter that is used to indicate the degree to which an explosive can be oxidized and thus an important criterion for selecting potential HEDCs. The value of OB in DNABT (-12.30%) close to CL-20 (-10.96%) maybe make for the heat releases in detonation by sufficient oxidation. Thus the fact that the heat of detonation of DNAT and DNABT as novel members are about 1310 cal/g and 1810 cal/g , which become the highest ones among all compounds including FOX-7 as well.

Detonation velocity and detonation pressure are two very important performance parameters for an energetic compound. As is evident in Table 5, both DNAT and DNABT show remarkable detonation parameters. The detonation velocity (9.17 km/s and 9.53 km/s) and detonation pressure (39.23 GPa and 40.92 GPa) are much greater than those of TNT, RDX and HMX as well as FOX-7. Overall, the detonation properties of both DNAT and DNABT are accordingly predicted to be second only to those of CL-20, and they might be the most powerful energetic materials among the CHNO-containing organic compounds.

4. Conclusion

Two novel members of FOX-7 family, 5-(dinitromethylene)-1,4-dinitramino-Tetrazole (DNAT) and 1,1'-dinitro-4,4'-diamino-5,5'-Bitetrazole (DNABT) have been proposed firstly.

The optimized structures are dominated by the planar tetrazole ring and carbon-carbon double bonds as well as many nitro and amino groups both in DNAT and DNABT molecules. And they are presumably stabilized by involving the lone pairs of alternate nitrogen and carbon atoms in distribution of electronic density. The electrostatic potentials are strongly positive above and below the central portions of the molecules while negative around the peripheries. The calculated thermochemical parameters, IR spectrum data have been performed for easier assignment and

positive identification of the target compounds. The predicted structures for four types of crystals including P_{212121} , $P_{21/C}$, $P-1$ and P_{BCA} , assigned to the orthorhombic, monoclinic and triclinic lattice systems, were optimized by using the first-principle plane-wave LDA density functional theory.

Two new molecules have higher density and the compound DNAT is up to $1.97 \text{ g}\cdot\text{cm}^{-3}$. Quite noteworthy in this respect are both of them with positive enthalpy of formation (583.50 kJ/mol and 1081.39 kJ/mol). It has been confirmed that DNAT and DNABT might be very promising energetic (catenated nitrogen atoms) and insensitive (tetrazole and FOX-7 fragments) compounds with eminent detonation properties (DNAT: $D = 9.17 \text{ km/s}$, $P = 39.23 \text{ GPa}$; DNABT: $D = 9.53 \text{ km/s}$, $P = 40.92 \text{ GPa}$), especially DNABT is equal to that of CL-20 ($D = 9.38 \text{ km/s}$, $P = 44.10 \text{ GPa}$).

Overall, a class of fascinating compounds as novel members of FOX-7 family, containing six or eight catenated nitrogen atom chains has been reported firstly. We expect that the relative theoretical work of such combination of energetic groups and insensitive fragments may open new methods for the synthesis of new high-nitrogen materials in the foreseeable future.

Acknowledgments

The support of the National Natural Science Foundation of China (Grant No. 10776002) is gratefully acknowledged.

References:

1. H. Gao and J. n. M. Shreeve, *Chem. Rev.*, 2011, 111, 7377-7436.
2. R. Wang, H. Xu, Y. Guo, R. Sa and J. n. M. Shreeve, *J. Am. Chem. Soc.*, 2010, 132, 11904-11905.
3. Q.-L. Yan, S. Zeman, J.-G. Zhang, P. He, T. Musil and M. Bartoskova, *Phys Chem Chem Phys.*, 2014.
4. Q. Zhang and J. M. Shreeve, *Angew Chem Int Ed Engl*, 2013, 52, 8792-8794.
5. Z. Yu and E. R. Bernstein, *J Phys Chem A*, 2013, 117, 1756-1764.
6. H. Xue, Y. Gao, B. Twamley and J. n. M. Shreeve, *Chem. Mater.*, 2005, 17, 191-198.
7. R. P. Singh, R. D. Verma, D. T. Meshri and J. M. Shreeve, *Angew Chem Int Ed Engl*, 2006, 45, 3584-3601.
8. T. M. Klapötke and C. M. Sabaté, *Chem. Mater.*, 2008, 20, 3629-3637.
9. Z. Liu, Q. Wu, W. Zhu and H. Xiao, *J. Phys. Org. Chem.*, 2013, 26, 939-947.
10. Q.-H. Lin, Y.-C. Li, C. Qi, W. Liu, Y. Wang and S.-P. Pang, *J. Mater. Chem. A*, 2013, 1, 6776.
11. T. M. Klapötke, P. Mayer, A. Schulz and J. J. Weigand, *J. Am. Chem. Soc.*, 2005, 127, 2032-2033.
12. T. M. Klapötke, F. A. Martin and J. Stierstorfer, *Chemistry*, 2012, 18, 1487-1501.
13. T. M. Klapötke, B. Krumm, F. A. Martin and J. Stierstorfer, *Chem Asian J*, 2012, 7, 214-224.
14. N. Fischer, T. M. Klapötke, M. Reymann and J. Stierstorfer, *Eur. J. Inorg. Chem.*, 2013, 2013, 2167-2180.
15. D. Fischer, T. M. Klapötke and J. Stierstorfer, *Propell. Explos. Pyrot.*, 2012, 37, 156-166.
16. D. Fischer, T. M. Klapötke, D. G. Piercey and J. Stierstorfer, *Chemistry*, 2013, 19, 4602-4613.
17. Z. P. Demko and K. B. Sharpless, *J. Org. Chem.*, 2001, 66, 7945-7950.
18. N. V. Latypov, J. Bergman, A. Langlet, U. Wellmar and U. Bemm, *Tetrahedron*, 1998, 54, 11525-11536.

19. W. A. Trzcinski, S. Cudziło, Z. Chylek and L. Szymanczyk, *J. Hazard. Mater.*, 2008, 34, 605-612.
20. D. E. Taylor, F. Rob, B. M. Rice, R. Podeszwa and K. Szalewicz, *Phys Chem Chem Phys.*, 2011, 13, 16629-16636.
21. B. Gao, P. Wu, B. Huang, J. Wang, Z. Qiao, G. Yang and F. Nie, *New J. Chem.*, 2014, 38, 2334-2341.
22. T. T. Vo, J. Zhang, D. A. Parrish, B. Twamley and J. n. M. Shreeve, *J. Am. Chem. Soc.*, 2013, 135, 11787-11790.
23. X. Song, J. Li, H. Hou and B. Wang, *J Comput Chem*, 2009, 30, 1816-1820.
24. J. Song, Z. Zhou, D. Cao, H. Huang, L. Liang, K. Wang and J. Zhang, *Z. Anorg. Allg. Chem.*, 2012, 638, 811-820.
25. M. M. Kuklja and S. N. Rashkeev, *Phys Rev B*, 2007, 75, 104111.
26. A. Hu, B. Larade, S. Dudi, H. Abou-Rachid, L.-S. Lussier and H. Guo, *Propell. Explos. Pyrot.*, 2007, 32, 331-337.
27. G. Hervé and G. Jacob, *Tetrahedron*, 2007, 63, 953-959.
28. G. Hervé, *Propell. Explos. Pyrot.*, 2009, 34, 444-451.
29. X. Song, J. Li, H. Hou and B. Wang, *J. Comput. Chem.*, 2009, 30, 1816-1820.
30. E. F. Byrd and B. M. Rice, *J. Phys. Chem. A*, 2006, 110, 1005-1013.
31. P. W. Atkins, *Physical Chemistry*, Oxford University Press, Oxford, 1982.
32. P. Politzer, J. S. Murray, T. Brinck and P. Lane, in *Immunoanalysis of Agrochemicals*, ACS Symp. Ser. 586, American Chemical Society, Washington, DC, 1994.
33. J. S. Murray and P. Politzer, in *Quantitative Treatment of Solute/Solvent Interactions, Theoretical and Computational Chemistry*, Amsterdam, 1994.
34. W. E. Pickett, *Computer Physics Reports*, 1989, 9, 117.
35. M. J. Kamlet and S. J. Jacobs, *J. Chem. Phys.*, 1968, 48, 23-35.
36. M. J. Frisch, G. W. Trucks, H. B. Schlegel, G. E. Scuseria, M. A. Robb, J. R. Cheeseman, J. A. Montgomery, Jr., T. Vreven, K. N. Kudin, J. C. Burant, J. M. Millam, S. S. Iyengar, J. Tomasi, V. Barone, B. Mennucci, M. Cossi, G. Scalmani, N. Rega, G. A. Petersson, H. Nakatsuji, M. Hada, M. Ehara, K. Toyota, R. Fukuda, J. Hasegawa, M. Ishida, T. Nakajima, Y. Honda, O. Kitao, H. Nakai, M. Klene, X. Li, J. E. Knox, H. P. Hratchian, J. B. Cross, V. Bakken, C. Adamo, J. Jaramillo, R. Gomperts, R. E. Stratmann, O. Yazyev, A. J. Austin, R. Cammi, C. Pomelli, J. W. Ochterski, P. Y. Ayala, K. Morokuma, G. A. Voth, P. Salvador, J. J. Dannenberg, V. G. Zakrzewski, S. Dapprich, A. D. Daniels, M. C. Strain, O. Farkas, D. K. Malick, A. D. Rabuck, K. Raghavachari, J. B. Foresman, J. V. Ortiz, Q. Cui, A. G. Baboul, S. Clifford, J. Cioslowski, B. B. Stefanov, G. Liu, P. Iiskorz, I. Komaromi, R. L. Martin, D. J. Fox, T. Keith, M. A. Al-Laham, C. Y. Peng, A. Nanayakkara, M. Challacombe, P. M. W. Gill, B. Johnson, W. Chen, M. W. Wong, C. Gonzalez and J. A. Pople, GAUSSIAN 9 (Revision A.01), Gaussian, Inc, 2009.
37. *Materials Studio*; San Diego; Accelrys Software Inc. 2008.
38. T. Lu and F. Chen, *J. Comput. Chem.*, 2012, 33, 580-592, <http://Multiwfn.codeplex.com>.
39. B. Kosar and C. Albayrak, *Spectrochim. Acta, Part A*, 2011, 78, 160-167.
40. J. S. Murray and P. Politzer, *Comp. Mol. Sci.*, 2011, 1, 153-163.
41. M. D. Segall, P. J. D. Lindan, M. J. Probert, C. J. Pickard, P. J. Hasnip, S. J. Clark and M. C. Payne, *J of Phys-Condens Mat*, 2002, 14, 2717-2744.
42. B. M. Rice, S. V. Pai and J. Hare, *Combust flame*, 1999, 118, 445-458.
43. P. Politzer and J. S. Murray, *Cent. Eur. J. Energ. Mater.*, 2011, 8, 209-220.